Bimanual Wearable EMG Control for Multi-Day In-Home Mobile Manipulation by a User with Quadriplegia

Jehan Yang
Carnegie Mellon University
Pittsburgh, Pennsylvania, USA

Eleanor Hodgson
Carnegie Mellon University
Pittsburgh, Pennsylvania, USA

Cindy Sun
Carnegie Mellon University
Pittsburgh, Pennsylvania, USA

Zackory Erickson*
Carnegie Mellon University
Pittsburgh, Pennsylvania, USA

Douglas J. Weber*
Carnegie Mellon University
Pittsburgh, Pennsylvania, USA

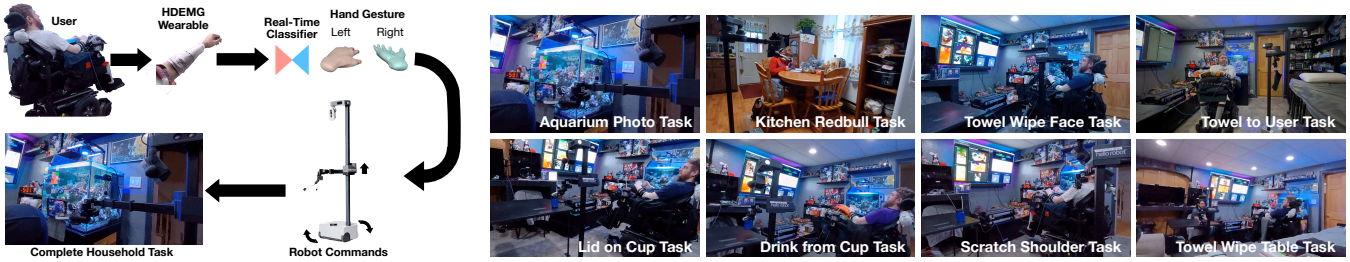

Figure 1: (Left) System overview showing a user with cervical spinal cord injury (cSCI) and limited wrist movements. electromyography (EMG) signals are classified on each forearm to infer user intent without requiring overt hand motion, and mapped to robot actions. (Right) Tasks performed in the user's home during the finalized study phase.

Abstract

Mobile manipulators in the home can enable people with cSCI to perform daily household tasks that they could not otherwise do themselves, yet paralysis often limits access to traditional control interfaces such as joysticks or keyboards. We introduce and deploy the first system that enables a user with quadriplegia to control a mobile manipulator in their own home using bimanual high-density electromyography (HDEMG). We develop custom fabric-integrated forearm sleeves worn on both arms that capture residual neuromotor activity and support real-time gesture-based robot control. We further integrate vision, language, and motion planning into a shared autonomy framework that assists with alignment and navigation while preserving user control. Finally, we present a twelve-day in-home user study demonstrating wearable EMG-based control of diverse activities of daily living (ADLs) and household tasks in a real home environment.

CCS Concepts

• **Human-centered computing** → **User studies**; • **Hardware** → *PCB design and layout*; • **Computing methodologies** → *Supervised learning by classification.*

Keywords

Assistive Robotics, Mobile Manipulation, Wearables, Shared Autonomy, Teleoperation, Users with Motor Impairments

ACM Reference Format:
Jehan Yang, Eleanor Hodgson, Cindy Sun, Zackory Erickson, and Douglas J. Weber. 2026. Bimanual Wearable EMG Control for Multi-Day In-Home Mobile Manipulation by a User with Quadriplegia. In *Proceedings of ACM/IEEE International Conference on Human-Robot Interaction (HRI '26).* ACM, New York, NY, USA, 9 pages. https://doi.org/XXXXXXX.XXXXXXX

1 Introduction

Millions of people live with quadriplegia, often caused by cSCI [1]. Loss of arm and trunk function can prevent independent performance of many ADLs such as feeding, drinking, hygiene, and object retrieval [7, 14], increasing reliance on caregivers. Mobile manipulators can extend assistive manipulation across a home, including when a user is seated in a wheelchair or lying in bed [13, 19]. A core barrier remains *control*: many existing interfaces assume hand, finger, or sustained head motion that may be difficult or fatiguing for users with quadriplegia.

Forearm EMG can capture residual neuromotor intent even when overt movement is absent [4, 18, 23, 27]. With HDEMG and learning-based algorithms, spatial activation patterns over the forearm can support reliable gesture decoding without precise electrode placement, enabling wearable, hands-free command channels. Prior work

*Both authors contributed equally to this research.

HRI '26, Edinburgh, UK

ACM ISBN 978-1-4503-XXXX-X/2018/06
https://doi.org/XXXXXXX.XXXXXXX

has demonstrated gesture decoding in individuals with paralysis, but has largely focused on offline decoding, laboratory settings, or single-arm sensing [4, 18, 23, 27]. In contrast, real-world assistive mobile manipulation introduces additional requirements: daily setup, robustness to sleeve shift and impedance changes, and safe online behavior under occasional misclassifications.

We present the first system that enables a user with clinically complete quadriplegia to control a mobile manipulator in their own home using *bimanual* fabric-integrated HDEMG. Each forearm sleeve contains 128 electrodes and supports real-time gesture classification. Gesture commands drive low-degrees of freedom (DOFs) teleoperation modes (base/arm, arm/gripper, wrist), while shared autonomy assists with perception, alignment, and navigation in situations where low-bandwidth control is most burdensome. We evaluate the full system in a twelve-day in-home deployment with a user with motor- and sensory-complete quadriplegia from cSCI: five exploratory days used to personalize gestures and stabilize online control, followed by seven standardized days with fixed configuration and repeated tasks (Fig. 1).

Contributions: (1) The first bimanual, fabric-integrated HDEMG forearm sleeves designed for real-time robot control in daily use. (2) A practical real-time pipeline for stable online gesture control under in-home variability. (3) A longitudinal twelve-day in-home case study demonstrating wearable HDEMG control of a mobile manipulator for ADLs and user-selected tasks, with quantitative task-time and subjective results.

2 Related Work

Assistive teleoperation interfaces. Assistive robot teleoperation has used joysticks, button-based controllers, and web interfaces [2, 20, 24]. Higher-bandwidth devices such as VR controllers or robotic arm "twins" can improve dexterity for able-bodied users [6, 8, 25] but remain inaccessible for many users with quadriplegia. Alternatives include sip-and-puff and mouth joysticks [3, 10] and brain–computer interfaces, which can require invasive sensing for continuous manipulation [9].

EMG and HDEMG neuromotor decoding. EMG-based interfaces can decode intended gestures from residual signals after paralysis [4, 18, 23, 27]. Robustness to inter-session variability and electrode shift is an ongoing challenge [5, 12, 26]. Many robustness strategies rely on large datasets or extended training, which conflicts with daily in-home use. Prior wearable EMG systems include rigid wristbands [21] and single-arm fabric sleeves for recognition [16].

Shared autonomy and in-home deployments. Shared autonomy reduces teleoperation burden through goal assistance, alignment support, action filtering, and mode switching [15, 19, 22]. A small number of studies have reported multi-day in-home deployments with users with motor impairments [11, 17, 19]. However, prior work in longitudinal in-home evaluations of wearable neuromotor interfaces paired with shared autonomy for mobile manipulation remains absent.

Figure 2: Flex PCB has 128 gold-plated electrodes soldered onto pads, folded and sewn into spandex fabric forearm sleeve, and attached onto both arms of the user. Three Velcro strips are also attached per sleeve in order to ensure electrodes make tight contact with the arm.

3 Wearable Bimanual HDEMG Interface

3.1 Sleeves and sensing

Each forearm sleeve integrates a flexible PCB into stretch fabric, providing 128 gold-plated electrodes per arm in an 8×16 grid (Fig. 2). The form factor emphasizes daily donning, comfort, and robustness to imprecise placement. The sleeves have their electrodes wiped between sessions with alcohol. Full fabrication diagrams and inner and outer sleeve layout views are provided in the Supplementary (Figs. 11–12).

3.2 Daily data collection and real-time decoding

Each day begins with cue-based data collection and a brief maximum voluntary contraction (MVC) calibration. EMG is filtered (20 Hz high-pass, 60 Hz notch), segmented into 80 ms windows with 40 ms stride, and converted into per-arm RMS spatial heatmaps. Separate lightweight convolutional neural networks (CNNs) are trained per arm to classify gestures from heatmaps. To support rapid daily retraining, the model is intentionally shallow; details (architecture, training, splits) appear in the Supplementary A.1.

3.3 Personalized gesture sets

Because residual neuromotor patterns vary substantially across individuals and across arms, we personalized the gesture vocabulary. The user screened candidate gestures and we selected a separable subset using average spatial heatmaps and cosine similarity. During the exploratory phase we evaluated a symmetric five-gesture set on both arms. Left-hand test accuracy was high while right-hand accuracy was lower. To improve online reliability, we reduced the right-hand vocabulary to three gestures for the standardized phase (Fig. 3). This reduced command diversity but improved stability for daily robot use. Confusion matrices for the five gesture vs three gesture classifier for the right hand is shown in Supplementary Fig. 9.

4 Teleoperation Pipeline and Online Stability

4.1 Real-time command generation

EMG is streamed from two Intan RHD2164 chips per arm to a companion laptop at 4,000 Hz (256 channels total), processed into heatmaps, and classified in real time. To prioritize safe online behavior over marginal offline accuracy, we smooth and gate classifier outputs before issuing motion commands. We apply an exponential moving average ($\alpha = 0.5$), a confidence threshold (0.75), and

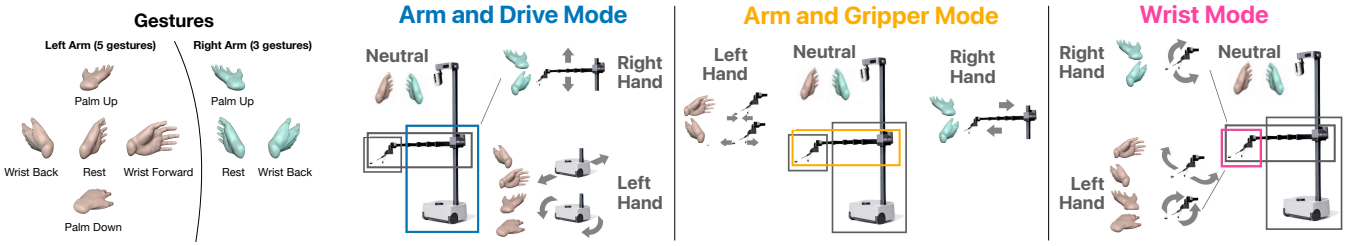

Figure 3: (Left) Gestures used for robot control on both hands for the last seven days. We decrease the number of gestures for the right hand due to lower classification accuracy on the right hand for this user. (Right) Gestures are mapped to robot movements in three different modes. Modes are cycled between either through voice commands ("Hey Robot, Next Mode") or holding the wrist back gesture on both hands for 0.2 seconds.

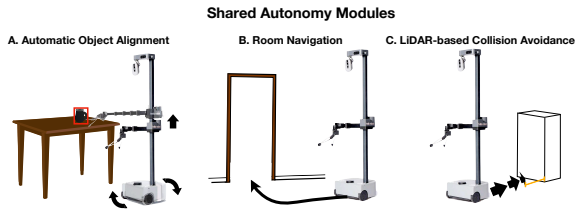

Figure 4: Illustrations of the three shared autonomy modules used: automatic object alignment, room navigation, and LiDAR-based collision avoidance.

majority voting over 11 predictions; commands are issued only if at least 6 of 11 agree, otherwise the output is treated as Rest. Robot commands are rate-limited to 10 Hz to suppress transient misclassifications.

4.2 User interface and modes

The user controls the robot through a web interface showing multiple camera views (head RGBD, wrist RGBD, wide-angle navigation) and predicted gestures. Gesture control is enabled/disabled via voice command. Gestures map to motion in three control modes: Arm+Drive, Arm+Gripper, and Wrist (Fig. 3). The standardized phase used a fixed set of camera feeds each day. The finalized GUI is shown in Supplementary Fig. 6

5 Shared Autonomy Modules

We include shared autonomy to reduce burden in situations where low-DOFs teleoperation is most difficult: fine alignment to objects, multi-room navigation, and safety during base motion (Fig. 4). Modules are activated by voice command and are designed to preserve user authority rather than executing full tasks autonomously.

5.1 Automatic object alignment

The user specifies a target object verbally. An open-vocabulary detector identifies the object in the head RGBD stream, estimates a 3D centroid, and an IK solver computes an alignment configuration. We adopt a driver-assistance style blending [19]:

$$\mathbf{u} = \mathbf{u}_h + \alpha \mathbf{u}_a, \tag{1}$$

where $\mathbf{u}_h$ is the user command, $\mathbf{u}_a$ is an autonomous alignment command, and $\alpha \in [0, 1]$ scales assistance based on system confidence. Assistance is constrained to coarse alignment and does not override user control of approach or grasp execution. The base rotation and arm height are commanded by $\mathbf{u}_a$.

5.2 Room navigation with gated autonomy

Room-level navigation is challenging when the robot is distant or outside the user's direct view. We pre-map the home and record goal coordinates for rooms. The Nav2 planner produces velocities $(v_{\text{nav}}, \omega_{\text{nav}})$ while the user provides directional intent via gestures. Forward progress is gated so the robot only advances along the planned path when the user explicitly commands forward motion, preserving continuous user control of motion onset and progress.

The user retains direct control over left and right turning gestures, which modulate or override the planner's rotational velocity, allowing coarse steering adjustments while following the path. A rest or reverse gesture immediately halts or backs the robot away from obstacles, respectively, ensuring that motion can be interrupted at any time. In this way, autonomy contributes path smoothing and goal-directed motion, while the user continuously governs direction, initiation, and interruption of movement in the case of mistakes by the module.

5.3 LiDAR-based collision monitor

A 2D LiDAR module runs continuously to scale base velocity near obstacles, smoothly stopping the robot as it approaches nearby objects during base forward and base backward commands. This reduces collision risk during teleoperation and navigation. No safety-critical collisions occurred in the deployment.

6 Twelve-Day In-Home Study

6.1 Participant and protocol

We conducted a twelve-day in-home deployment with a 39 year-old male with a C5 cSCI and AIS A (motor- and sensory-complete quadriplegia), 19 years post injury. The user had no prior experience controlling a mobile manipulator in his home. Days 1–5 were exploratory: we collected EMG data, evaluated daily training needs, performed practice tasks (Supplementary Fig. 13), and refined online interface elements. Days 6–12 used a standardized configuration with a personalized right-hand gesture set (three gestures). Shared autonomy was introduced incrementally during the standardized phase: object alignment on Day 9 and room navigation on Day 11.

6.2 Tasks

Tasks spanned ADLs, instrumental ADLs, and a user-selected leisure task: drinking from a cup, placing a lid, wiping surfaces, retrieving objects from another room, and picture taking. The cup-drinking task was repeated daily during the standardized phase to measure learning over time. Full task setups appear in Supplementary B.

7 Results

7.1 Task times and learning over days

Across the deployment, the user performed 11 distinct tasks (8 during the standardized phase), with task completion times ranging from 124–754 s (Fig. 5). For the repeated cup task, a least-squares trend line shows a decrease of approximately 33 s/day under pure teleoperation (Fig. 5), consistent with user learning and increased familiarity. A Spearman rank correlation did not show a statistically significant monotonic trend under pure teleoperation ($\rho = -0.14$, $p = 0.38$, $n = 7$), so we interpret trends descriptively.

7.2 Effects of shared autonomy

When object alignment was enabled for the cup task, task time decreased more steeply (least-squares trend of approximately 55 s/day across the three shared-autonomy trials), and trial-to-trial variability was substantially lower than pure teleoperation (Supplementary Fig. 7). For navigation-heavy tasks requiring multi-room traversal and distant alignment, shared autonomy provided the largest time benefit. For the Energy Drink Kitchen task, Align+Room Mode reduced completion time relative to teleoperation (Tab. 1), though the number of trials is small and results are interpreted for feasibility.

In-home deployment exposed open-vocabulary perception failure modes not commonly surfaced in lab settings. For example, in Lid on Cup, the detector initially misidentified the cup as the lid due to the bicolor cup appearance and camera field of view, increasing task time in that trial. The user recovered by attempting other language queries and by repositioning camera. Over successive sessions, the user adapted by positioning target objects within view and issuing more specific language queries (e.g., "energy drink" vs. "can"), highlighting co-adaptation between user and system as a factor in perception-driven assistance.

7.3 Gesture classification accuracy and online robustness

Daily held-out test accuracies varied across days (Fig. 8; full confusion matrices in Supplementary). During the standardized phase, mean test accuracy was 90.9% ± 5.3% for the left hand and 98.0% ± 2.0% for the right hand under the reduced three-gesture configuration. We did not find a significant association between daily test accuracy and cup task time ($\rho = -0.21$, $p = 0.34$, $n = 7$), suggesting that online stability mechanisms (temporal filtering, confidence gating) and user learning can matter more for real-world teleoperation than marginal gains in offline accuracy.

7.4 Subjective results

The user donned the sleeves with minor preparation. Recalibration occurred opportunistically when online performance degraded (median two times per day), most often due to sleeve shift. Usability and workload measured with system usability score (SUS) and a modified 7-point NASA-TLX were favorable, with increasing usability and decreasing workload over days (Appendix Fig. 10). By the final study day, shared autonomy achieved lower task times with comparable workload and higher usability than pure teleoperation.

Table 1: Energy Drink Kitchen task times comparing pure teleoperation and align + room mode.

Condition	Avg. Time (s)	Trials (n)
Pure Teleoperation	738	1
Align + Room Mode	517 ± 62	2

8 Discussion and Limitations

This deployment suggests three practical design implications for wearable neuromotor assistive control. First, personalization can be more effective than a fixed "maximal" gesture vocabulary: reducing the right-hand gesture set improved reliability. Second, without impairment-specific large datasets, rapid retraining is more compatible with in-home variability for a user with a motor impairment than pretraining approaches for EMG gesture recognition. Third, shared autonomy benefits are task- and training-dependent: manual alignment can become efficient with continuous camera feedback and repetition, while navigation-heavy or distant alignment tasks benefit more from autonomy.

9 Conclusion

We present the first in-home deployment in which a user with clinically complete quadriplegia controls a mobile manipulator using bimanual, fabric-integrated HDEMG sleeves. A real-time pipeline emphasizing online stability enabled daily gesture-based teleoperation, and shared autonomy supported alignment and navigation in an unstructured home. In a twelve-day deployment, the user completed diverse household and personalized tasks, with improved task efficiency over repeated use and favorable subjective usability and workload. These results support wearable neuromotor interfaces, paired with task-appropriate shared autonomy, as a practical path toward daily in-home assistive mobile manipulation.

Acknowledgments

This work was supported by the National Science Foundation under Grant No. 2341352.

References

[1] Brian S Armour, Elizabeth A Courtney-Long, Michael H Fox, Heidi Fredine, and Anthony Cahill. 2016. Prevalence and causes of paralysis—United States, 2013. *American journal of public health* 106, 10 (2016), 1855–1857.

[2] Patrik Björnfot. 2021. Evaluating Input Devices for Robotic Telepresence. In *Proceedings of the 32nd European Conference on Cognitive Ergonomics*. ACM, Siena, Italy, 1–8.

[3] José Cláudio da Silva Junior and Walter Germanovix. 2019. Development of a sip-and-puff interface for communication and control of devices. In *Latin American Conference on Biomedical Engineering*. Springer, Springer, Cancun, Mexico, 1137–1146.

[4] Dailyn Lisbeth Despradel Rumaldo, Maxwell Murphy, Luigi Borda, Najja Marshall, Emanuele Formento, Mario Bracklein, JinHyung Lee, Jun Ye, Peter Walkington, Dano Morrison, et al. 2026. Enabling Skilled Human-Computer Interaction After Paralysis via a Wearable sEMG Interface. *bioRxiv* 10.64898/2026.01.09.698484, 1 (2026), 2026–01.

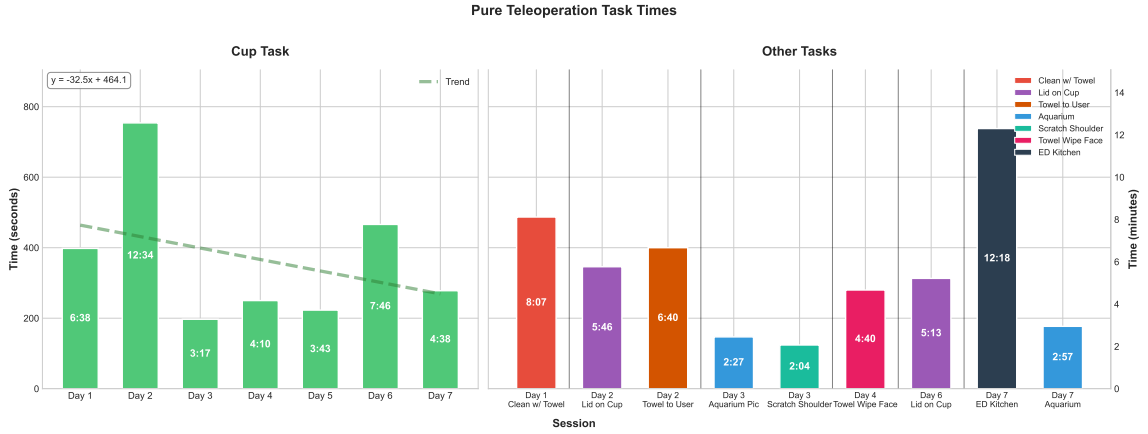

Figure 5: Task times for all tasks performed over the second week. (Left) Task times for cup task performed over the second week. This task is repeated each day. A least-squares trend line is shown, indicating a decrease of approximately 33 seconds per day. (Right) Task times for other tasks performed over the second week.

[5] Yu Du, Wenguang Jin, Wentao Wei, Yu Hu, and Weidong Geng. 2017. Surface EMG-based inter-session gesture recognition enhanced by deep domain adaptation. *Sensors* 17, 3 (2017), 458.

[6] Zipeng Fu, Tony Zhao, and Chelsea Finn. 2024. Mobile ALOHA: Learning Bimanual Mobile Manipulation with Low-Cost Whole-Body Teleoperation. *ArXiv* abs/2401.02117 (2024), 20 pages. https://api.semanticscholar.org/CorpusID:266755740

[7] K Whalley Hammell. 2004. Exploring quality of life following high spinal cord injury: a review and critique. *Spinal cord* 42, 9 (2004), 491–502.

[8] Zheyuan Hu, Robyn Wu, Naveen Enock, Jasmine Li, Riya Kadakia, Zackory Erickson, and Aviral Kumar. 2025. RaC: Robot learning for long-horizon tasks by scaling recovery and correction. *arXiv preprint arXiv:2509.07953* 2509.07953, 1 (2025), 26 pages.

[9] Christopher Hughes, Angelica Herrera, Robert Gaunt, and Jennifer Collinger. 2020. Bidirectional brain-computer interfaces. *Handbook of clinical neurology* 168 (2020), 163–181.

[10] Xueliang Huo, Jia Wang, and Maysam Ghovanloo. 2008. Introduction and preliminary evaluation of the Tongue Drive System: wireless tongue-operated assistive technology for people with little or no upper-limb function. *Journal of Rehabilitation Research & Development* 45, 6 (2008), 12 pages.

[11] Rajat Kumar Jenamani, Tom Silver, Ben Dodson, Shiqin Tong, Anthony Song, Yuting Yang, Ziang Liu, Benjamin Howe, Aimee Whitneck, and Tapomayukh Bhattacharjee. 2025. FEAST: A Flexible Mealtime-Assistance System Towards In-the-Wild Personalization. *arXiv preprint arXiv:2506.14968* 2506.14968, 2 (2025), 29 pages.

[12] Patrick Kaifosh and Thomas R Reardon. 2025. A generic non-invasive neuromotor interface for human-computer interaction. *Nature* 645, 8081 (2025), 702–711.

[13] Charles C Kemp, Aaron Edsinger, Henry M Clever, and Blaine Matulevich. 2022. The design of stretch: A compact, lightweight mobile manipulator for indoor human environments. In *2022 International Conference on Robotics and Automation (ICRA)*. IEEE, IEEE, Philadelphia, PA, USA, 3150–3157.

[14] Chih-Ying Li, Craig Velozo, Ickpy Hong, and Jill Newman. 2017. Longitudinal Change in Activities of Daily Living for Persons With Spinal Cord Injury Across 20 Years. *The American Journal of Occupational Therapy* 71, 4_Supplement_1 (2017), 7111500010p1–7111500010p1.

[15] Dylan P Losey, Hong Jun Jeon, Mengxi Li, Krishnan Srinivasan, Ajay Mandlekar, Animesh Garg, Jeannette Bohg, and Dorsa Sadigh. 2022. Learning latent actions to control assistive robots. *Autonomous robots* 46, 1 (2022), 115–147.

[16] Eric C Meyers, David Gabrieli, Nick Tacca, Lauren Wengerd, Michael Darrow, Bryan R Schlink, Ian Baumgart, and David A Friedenberg. 2024. Decoding hand and wrist movement intention from chronic stroke survivors with hemiparesis using a user-friendly, wearable EMG-based neural interface. *Journal of Neuro-Engineering and Rehabilitation* 21, 1 (2024), 7.

[17] Amal Nanavati, Ethan K Gordon, Taylor A Kessler Faulkner, Yuxin Ray Song, Jonathan Ko, Tyler Schrenk, Vy Nguyen, Bernie Hao Zhu, Haya Bolotski, Atharva Kashyap, et al. 2025. Lessons Learned from Designing and Evaluating a Robot-Assisted Feeding System for Out-of-Lab Use. In *2025 20th ACM/IEEE International Conference on Human-Robot Interaction (HRI)*. IEEE, IEEE, Melbourne, Australia, 696–707.

[18] Daniela Souza Oliveira, Matthias Ponfick, Dominik I Braun, Marius Osswald, Marek Sierotowicz, Satyaki Chatterjee, Douglas Weber, Bjoern Eskofier, Claudio Castellini, Dario Farina, et al. 2024. A direct spinal cord–computer interface enables the control of the paralysed hand in spinal cord injury. *Brain* 147, 10 (2024), 3583–3595.

[19] Akhil Padmanabha, Janavi Gupta, Chen Chen, Jehan Yang, Vy Nguyen, Douglas J Weber, Carmel Majidi, and Zackory Erickson. 2024. Independence in the home: A wearable interface for a person with quadriplegia to teleoperate a mobile manipulator. In *Proceedings of the 2024 ACM/IEEE International Conference on Human-Robot Interaction*. ACM/IEEE, Boulder, Colorado, USA, 542–551.

[20] Vinitha Ranganeni, Noah Ponto, and Maya Cakmak. 2023. Evaluating customization of remote tele-operation interfaces for assistive robots. In *2023 32nd IEEE International Conference on Robot and Human Interactive Communication (RO-MAN)*. IEEE, IEEE, Busan, South Korea, 1633–1640.

[21] Mithileysh Sathiyanarayanan and Sharanya Rajan. 2016. MYO Armband for physiotherapy healthcare: A case study using gesture recognition application. In *2016 8th International Conference on Communication Systems and Networks (COMSNETS)*. IEEE, IEEE, Bangalore, India, 1–6.

[22] Yiran Tao, Jehan Yang, Dan Ding, and Zackory Erickson. 2025. LAMS: LLM-Driven Automatic Mode Switching for Assistive Teleoperation. In *2025 20th ACM/IEEE International Conference on Human-Robot Interaction (HRI)*. IEEE, ACM/IEEE, Melbourne, Australia, 242–251.

[23] Jordyn E Ting, Alessandro Del Vecchio, Devapratim Sarma, Nikhil Verma, Samuel C Colachis 4th, Nicholas V Annetta, Jennifer L Collinger, Dario Farina, and Douglas J Weber. 2021. Sensing and decoding the neural drive to paralyzed muscles during attempted movements of a person with tetraplegia using a sleeve array. *Journal of neurophysiology* 126, 6 (2021), 2104–2118.

[24] Kay N Wojtowicz and Maria E Cabrera. 2023. Stretch to the Client; Re-imagining Interfaces. In *Companion of the 2023 ACM/IEEE International Conference on Human-Robot Interaction*. ACM/IEEE, Stockholm, Sweden, 891–892.

[25] Philipp Wu, Yide Shentu, Zhongke Yi, Xingyu Lin, and Pieter Abbeel. 2024. Gello: A general, low-cost, and intuitive teleoperation framework for robot manipulators. In *2024 IEEE/RSJ International Conference on Intelligent Robots and Systems (IROS)*. IEEE, IEEE, Abu Dhabi, UAE, 12156–12163.

[26] Jehan Yang, Maxwell Soh, Vivianna Lieu, Douglas J Weber, and Zackory Erickson. 2024. EMGBench: benchmarking out-of-distribution generalization and adaptation for electromyography. *Advances in Neural Information Processing Systems* 37 (2024), 50313–50342.

[27] Xingchen Yang, Daniela Souza De Oliveira, Dominik I Braun, Matthias Ponfick, Dario Farina, and Alessandro Del Vecchio. 2025. Non-Invasive Neural Interfacing for Tetraplegic Individuals Using Residual Motor Neuron Activity Decoded At the Forearm or Wrist. *IEEE Journal of Biomedical and Health Informatics* 29, 10 (2025), 9 pages.

A Supplementary

A.1 Data Collection Details and Classifier

During data collection, the user performs gestures using a cueing-based protocol. Each trial begins with a visual cue indicating the next gesture for 3 seconds, followed by a 5-second hold period during which the user attempts to perform the gesture. To account for variable reaction times, we use the final 4 seconds of each hold

period as training data. At the beginning of each session, the user performs each gesture once at maximum voluntary contraction (MVC) to initialize an RMS-based calibration.

EMG signals are processed using a 20 Hz high-pass filter and a 60 Hz notch filter to remove motion artifacts and powerline noise. We then compute the RMS value for each channel. For real-time feedback, we use the 90th percentile of RMS values across the 128 channels, which provides a robust measure of activation for gestures that may be spatially localized due to residual motor unit activity. This feedback is displayed to the user during data collection to help regulate effort.

To encourage consistent signal quality, data collection sessions alternate between target effort ranges of 15–30% and 20–40% of the MVC RMS. Each session consists of five sets, with three repetitions of each gesture per set. Depending on the day, the user completes between two and six data collection sessions. When online classification performance degrades during robot control, typically due to sleeve shift or changes in skin impedance, additional data collection sessions are performed at the researcher's discretion, collecting data from gestures with the lowest online accuracy.

For classifier evaluation, we reserve the final 10% of trials for each gesture as a held-out test set, enabling evaluation of generalization across time and across repeated gesture attempts. The remaining data is shuffled and split into training and validation sets using a 75/25 split. To accommodate daily time constraints during the study, classifiers are trained for three epochs. The model with the lowest validation cross-entropy loss is selected for real-time robot control. Samples are generated from splitting data into 80 ms windows with a 40 ms stride length.

The CNN consists of two 2D convolutional layers with 3×3 kernels and 128 filters, followed by batch normalization and ReLU activations. The resulting features are flattened and passed through a 128-node fully connected layer for classification. We intentionally use a lightweight RMS-based representation and shallow CNN to enable rapid retraining and real-time inference on a companion laptop, prioritizing deployability over maximal offline accuracy.

A.2 Graphical User Interface

The graphical user interface displayed to the user is shown in Supplementary Figure 6. On the left side of the interface, the user sees the camera feeds, including both color and depth images. All three cameras on the Stretch robot are used: the RGBD cameras on the head and wrist, as well as the head-mounted fisheye camera.

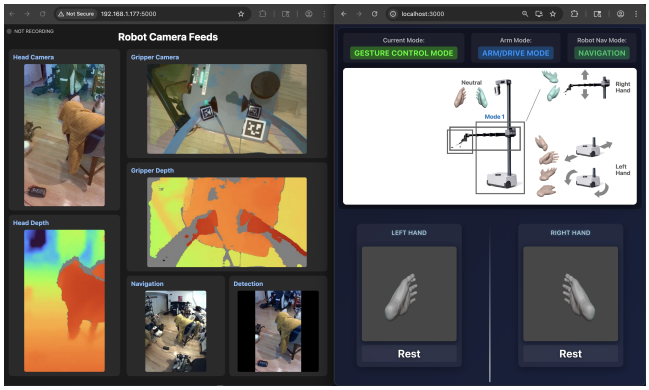

Figure 6: GUI showing camera feeds from the robot, mode mappings, and currently predicted gestures on both hands

A.3 Task Time Variability Under Shared Autonomy

Figure 7 provides a focused comparison of the final three sessions of the repeated cup task, contrasting pure teleoperation with automatic object alignment. While both conditions exhibit reduced task time relative to earlier sessions, shared autonomy shows lower session-to-session variability. These results are descriptive due to the small number of repetitions but illustrate the consistency benefit observed during repeated use of the alignment feature.

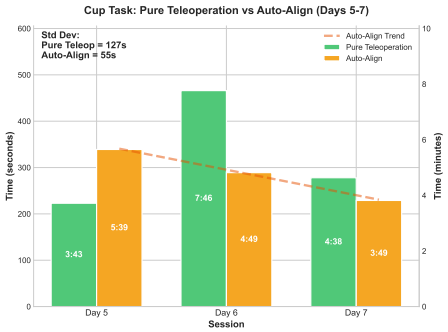

Figure 7: Task times comparing pure teleoperation with auto-align. Auto-alignment shows a visually consistent decrease in task time, while pure teleoperation exhibits higher variability.

A.4 Daily Gesture Classification Accuracy

Figure 8 reports held-out test accuracies for gesture classification across both study weeks. During the exploratory phase (Week 1), right-hand accuracy was consistently lower than left-hand accuracy, motivating the reduction of the right-hand gesture vocabulary for the finalized phase. Following this personalization, right-hand accuracy increased and remained stable across sessions. These trends highlight the role of personalized gesture selection in maintaining reliable real-time control for a user with motor impairment from cervical spinal cord injury.

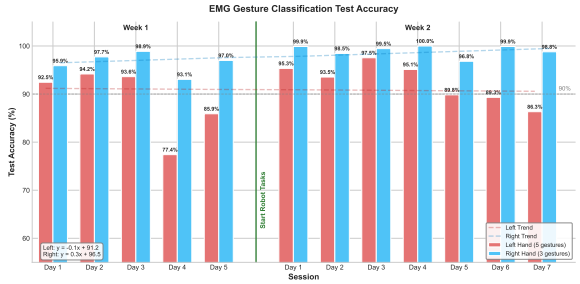

Figure 8: Test accuracies per day for week 1 and week 2.

Figure 9 presents average confusion matrices for five-gesture classification on each hand and the reduced three-gesture classifier on the right hand. The right-hand five-gesture configuration exhibited greater confusion between wrist flexion and wrist pronation, consistent with the user's limited observable range of motion for these gestures. Reducing the right-hand gesture set improved separability and overall classification reliability, as seen in right hand test accuracies (Fig. 8).

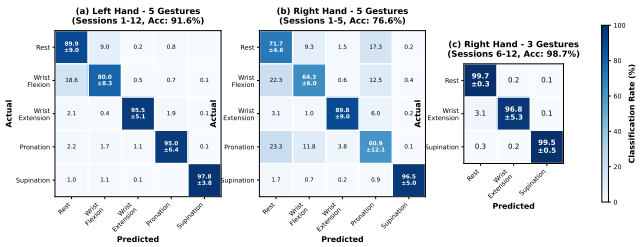

Figure 9: Average confusion matrices for classification for 5 gestures on each hand and 3 gestures on the right hand.

A.5 Subjective Usability and Workload

Figure 10 summarizes subjective usability and perceived workload for the repeated cup task using the System Usability Scale (SUS) and a 7-point NASA-TLX workload score. Usability scores generally increased across sessions, while workload scores decreased, indicating improved familiarity with the interface. Differences between pure teleoperation and shared autonomy were modest but show a tendency toward higher usability under shared autonomy in later sessions.

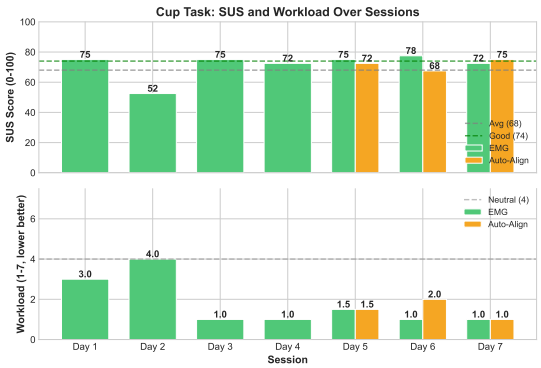

Figure 10: (Top) SUS of cup task comparing teleoperation vs shared mode. Reference lines correspond to standard SUS interpretive thresholds. (Bottom) 7-point Likert-style median NASA-TLX workload score of cup task for teleoperation vs shared mode.

A.6 Sleeve Hardware Layout

Figures 11 and 12 illustrate the inner and outer construction of the fabric-integrated HDEMG sleeves. The inner surface contains 128 gold-plated electrodes arranged to contact the forearm, while the outer surface exposes connectors for attachment to the Intan RHD2164 headstage. This layout enables high-density sensing while maintaining a wearable textile form factor suitable for daily donning and doffing with a single zipper.

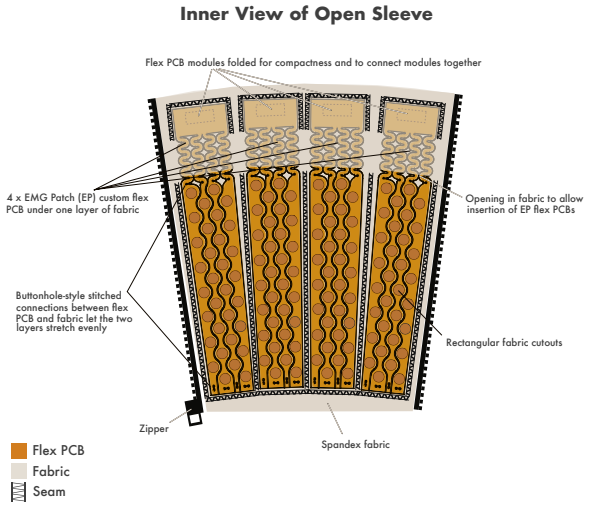

Figure 11: Inner view of diagram for sleeve. The 128 gold-plated electrodes are on this side and make contact with the skin.

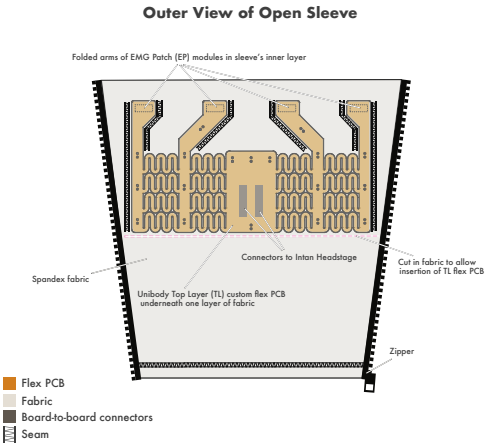

Figure 12: Outer view of diagram for sleeve. The center shows the connectors used to connect to the Intan RHD 2164 headstage.

B Task Setup and Description

(1) Drink from Cup
- Setup: A cup of water with a straw is placed on a table to the left of the user's wheelchair.
- Description: The user has to drive the robot towards the cup, grab the cup, and then bring the cup to their face. Because the height of the robot is lower than the user's face in his wheelchair, the robot needs to angle up the wrist and roll the wrist in order to locate the end of the straw around the user's mouth. The task is considered finished when the user drinks from the cup.

(2) Lid on Cup
- Setup: A cup and a lid is placed on a table next to the user.
- Description: The user has to pick up the lid that is flat on the table, then place the lid on the cup. The task is considered finished when the lid is placed on the cup and pressed onto the cup.

(3) Scratch Shoulder
- Setup: The robot is placed to the left of the user.
- Description: The user has to drive the robot to the user and place pressure with the gripper on the user's shoulder. The task is considered finished when the user has made contact with the robot and rubbed their shoulder with the towel.

(4) Towel Wipe Table
- Setup: The robot holds a small black towel in its gripper. Five pieces of red masking tape are placed on the table within a small square.
- Description: The user has to remove the five pieces of red tape from the table using the towel in the robot's gripper. The task is considered finished when the pieces of tape are no longer on the table.

(5) Energy Drink Kitchen
- Setup: The robot starts in the user's bedroom near the doorway. An energy drink is placed on the table in the kitchen.
- Description: The user has to drive the robot out of the room, through a hallway, and into the kitchen. The robot has to grab the energy drink and pick up the drink. The task is considered finished when the drink is picked up.

(6) Towel Wipe Face
- Setup: A small black hand towel is placed folded on a table to the left of the user.
- Description: The user has to grab the towel and bring the towel to the user's face with the robot. The task is considered finished when the user wipes their face using the hand towel.

(7) Bring Towel to User
- Setup: A large towel typically used for cushioning by the user is placed on the bed of the user.
- Description: The user has to bring the towel to the user with the robot. The task is considered finished when the user is able to take the towel from the robot, which is used for cushioning for the user.

(8) Aquarium Photo
- Setup: The robot is moved to the right of the aquarium with an iPad Mini placed in the gripper of the robot. The camera app is opened on the iPad mini.
- Description: The user has to bring the tablet and point it toward the aquarium. The task is considered finished when the user is able to take a picture of the aquarium using voice commands.

C Practice Tasks Setup and Description

(1) Drink from Cup
- Setup: Same as in Section B.
- Description: Same as in Section B.

(2) Turn Off Light
- Setup: The robot is placed near the light switch.
- Description: The user has to use the robot to turn off the light. The gripper has to tap the light switch and the task is considered finished when the light has been turned off.

(3) Adjust Curtains
- Setup: The curtains are open, which lets in light into the bedroom.
- Description: The user has to use the robot to grab the curtain and slide the curtain to partially close the curtain. The task is considered finished when the user has grabbed the curtain and moved it any distance to partially close the curtain.

(4) Open Door
- Setup: The door is closed and the robot is placed near the door. The user tested with joystick control for only this task.
- Description: The user has to open the door. The task is considered finished when the robot has opened the door and pushed it open to a 45 degree angle.

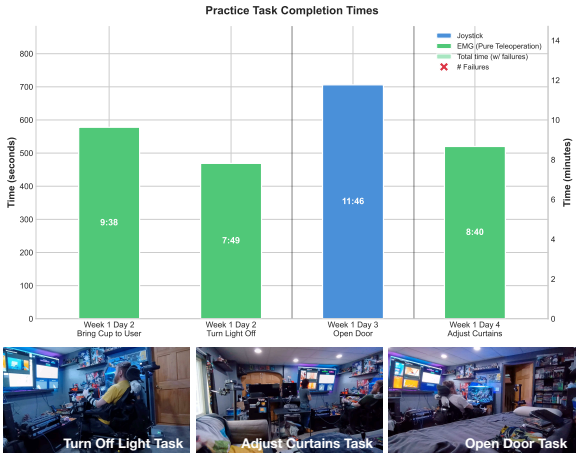

Figure 13: Additional tasks performed in the first week as practice tasks. In this week, we tested using 5-gesture classifiers in each hand, using only RGB camera feeds without a fisheye lens camera, and tested using a joystick for control. We found that the camera feed was also unreliable, but was fixed by switching the internet browser used in the second week.

Received 16 February 2026; accepted 2 March 2026